

Study of the Dimensional Instabilities of Laminated Polypropylene Films During Heating Treatments

M. Ponçot,^{1,2} J. Martin,¹ J. M. Hiver,¹ D. Verchère,² A. Dahoun¹

¹IJL Département SI2M—UMR 7198 CNRS—Nancy Université/Ecole Nationale Supérieure des Mines de Nancy, Parc de Saurupt, 54042 Nancy Cedex, France

²ArcelorMittal R&D Automotive Applications Montataire, BP 30109, 1 Route de Saint Leu, 60761 Montataire Cedex, France

Received 18 December 2009; accepted 4 November 2011

DOI 10.1002/app.36450

Published online in Wiley Online Library (wileyonlinelibrary.com).

ABSTRACT: Ensuring the geometrical stability of organic coatings is a key challenge for steel/polymer composites produced by the automotive industry to reduce the cars' weight. During the thermal treatment of painting, which exceeds the melting temperature of the organic part of the laminated film, polymer shrinkage may occur. It induces uncovered parts of the steel sheet which would present negative corrosion behavior in use. Two original and innovative experiments were presented. They enable to measure the deformation induced by the shrinkage and then to identify the microstructural mechanisms responsible for its appearance. Main results show strong influences of the macromolecular chains orientation induced by the

film extrusion process and of the postheating parameters used to perform the painting curing. Raman spectroscopy and differential scanning calorimetry are used both to perform analysis of the microstructure evolution during heating treatments in terms of crystals melting, crystalline macromolecular chains disorientation, and volume damage healing. © 2012 Wiley Periodicals, Inc. *J Appl Polym Sci* 000: 000–000, 2012

Key words: polypropylene films; shrinkage; video-metric measurements; heating treatment; macromolecular orientation; volume damage; melting disorientation; Raman spectroscopy

INTRODUCTION

The control of the dimensional instabilities of laminated polymer on steel is a key challenge for these composites essentially produced for the automotive industry. The lamination step occurs between a polymer film roll and a hot metal coil. The transformation in car bodywork parts passes through hard processes in terms of mechanical and thermal solicitations. First, stamping occurs, which induces high deformation zones where the microstructure of the organic layer is locally modified. Many authors frequently report macromolecular chains orientation along the mechanical axis^{1–6} and volume damage development^{1,5,7} in case of stretched polymers such as polyolefins. In our case, the material studied is an impact polypropylene. After assembling, the vehicle undergoes the painting treatment, also called the cathoresis process. It consists the curing of pieces in an oven at 200°C for about 20 min. This temperature is higher than the melting temperature of the polypropylene film. As a consequence, shrinkage occurs

while the polymer microstructure is changing. Uncovered bear parts of the steel sheet are then involved which enables negative corrosion behavior.

In the literature, previous studies are focused on the polypropylene shrinkage phenomenon. Unfortunately, attention was essentially laid on moulding shrinkage^{8–10} at the time of the injection process. A great dependence of the machining parameters was shown in terms of temperatures profile, matter flow rate, and pressures. In general, we may discern three types of injection moulding shrinkage¹⁰: (i) in-mould shrinkage (during processing, it may show up only in extreme cases), (ii) as-moulded shrinkage (shrinkage just after the mould opening, sometimes referred to as “mould shrinkage”), and (iii) postshrinkage (time effects during storage as physical aging, recrystallization, chains relaxation, etc.). Jansen et al.¹⁰ showed that all shrinkage data is well described by a simple equation that relates shrinkage to the local pressure history in the case of PS, ABS, HIPS, PC, PBT, and HDPE. Only a few studies were realized in the past on polypropylene and polyethylene films processed by extrusion.^{2–4,11,12} The melt (extrusion) and solid state (drawing) deformations were overviewed and all the authors showed the importance of the induced macromolecular chains orientation on the shrinkage measurement. Amorphous and crystalline orientations are

Correspondence to: M. Ponçot (marc.poncot@mines.inpl-nancy.fr).

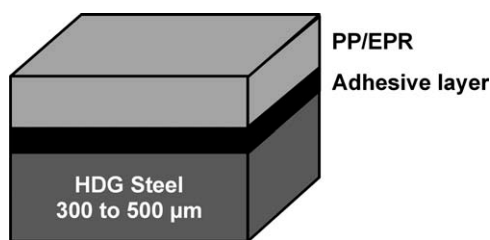


Figure 1 Typical cut of studied composite along its thickness.

responsible for the films shrinkage when temperature approaches the polymer melting point because of the chains tendency to recover their initial conformations: amorphous random coil and crystalline spherulites. Vries et al.² demonstrated the poor influence of the amorphous orientation in the shrinkage magnitude. As a consequence, during heating above the melting temperature, polymer films' geometrical instabilities overcome mainly from the crystalline phase.

This manuscript presents two original and innovative experiments elaborated at the laboratory to enable the quantification and the identification of the microstructural mechanisms of the polymer films shrinkage upon various heating treatments. The first one follows *in situ* the phenomenon thanks to dots markers displacements previously and judiciously disposed on the surface of the polymer layer. The important effect of the heating mode on the geometrical instabilities magnitude is studied using a thermoregulated heating plate and samples presenting macromolecular chains orientation induced by the extrusion process. Influences of a predeformation at a constant true deformation rate are then exposed since such kind of solicitation mainly induces microvoids when impact polypropylene is filled with mineral fillers.^{1,13} Involved micromechanisms are identified and described in terms of crystalline macromolecular chains disorientation and cavities healing. This way, a second system is developed using a Raman micro-spectrometer instead of the video control measurement equipment.

MATERIALS AND EXPERIMENTAL SETUP

Materials

The material studied here is a bi-layered polymer film being part of multilayered composite described in Figure 1. Each of the organic film presents an isotactic polypropylene main matrix. It exhibits an attractive combination of low cost, low weight, and extraordinary versatility in terms of properties, applications, and recyclability.¹⁴ The first layer in contact with the hot dipped galvanized steel is a copolymer ethylene-propylene grafted by maleic anhy-

dride lateral groups. This functionalized polymer called adhesive layer in the rest of this article ensures the adhesion between treated steel surface and the superior polymer layer. This second film is an impact polypropylene. It means that the isotactic polypropylene main matrix is filled with ethylene propylene rubber particles. Furthermore, a low amount of mineral fillers is incorporated. This material will be mentioned as PP/EPR in the rest of this article. The melting temperatures measured by differential scanning calorimetry of these two polymer layers are 135 and 167°C at 10°C min⁻¹, respectively.¹

Two types of bi-layered polymer films are studied here and they are called Films A and B. Their process and microstructure descriptions are listed in the Table I. $F_{(040)/1}$ is the orientation Hermans factor of the crystal family planes (040) of the iPP α phase in function of the extrusion flow direction, I .¹⁵ L_c is the crystalline lamellae thickness in nanometer calculated thanks to small angle X-rays scattering results. χ_c is the amount of crystallization of the polymer films obtained by wide angle X-rays scattering in transmission mode.¹⁶ Film A shows an important initial crystalline orientation in the extrusion flow direction involved by calendering (the cooling postextrusion process). On the contrary, Film B postextrusion process is cast and the well chosen experimental parameters set does not induce prior macromolecular chains orientation compared to Film A.

Samples preparation

Two geometries of samples are used depending on the considered study. In case of materials without previous mechanical solicitation, which means that specific microstructure is only induced by the conformation process (extrusion, postextrusion cooling, and colamination on treated steel), the sample geometry is presented in Figure 2(a). Clean cuts of the upper organic layer are done using a thin razor blade. It is necessary to ensure an extrusion flow direction length of at least 15 mm, because a sample size study shows that, in case of oriented organic film, polymer shrinkage induces displacements until the seventh millimetre from the extreme edge.¹ Consequently, the usual sample size is 30 × 30 mm² since the phenomenon is symmetrical.

TABLE I
Microstructural Datas of the Studied Bi-Layered Polypropylene Films

Films names	Postextrusion mode	$F_{(040)/1}$	L_c (nm)	χ_c (%)
A	Calendering	-0.22	9	43
B	Cast	-0.06	9.6	48

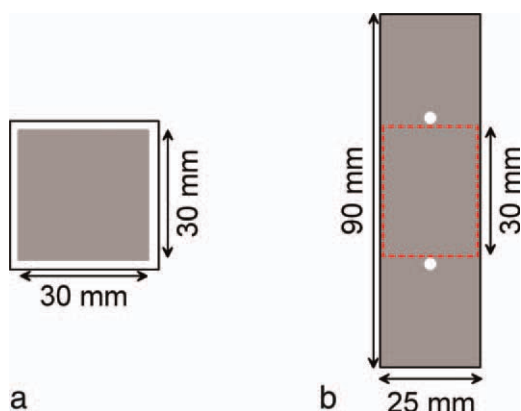


Figure 2 (a) Sample dimensions used to study influences of macromolecular orientation induced by the conformation processes. (b) Sample dimensions used to study deformation influences on shrinkage magnitude. [Color figure can be viewed in the online issue, which is available at wileyonlinelibrary.com.]

For the analysis of the influences of a sample pre-deformation in tension, the geometry used to perform selected true deformation values is illustrated in Figures 2(b) and 3 before and after stretching, respectively. Then a zone is delimited just between the two dots markers to be used for the shrinkage test. Length is 30 mm. Width measures about 25 mm \pm 0.1 mm depending on the deformation magnitude. In case of deformed samples, the whole sample presents always displacements due to the homogeneous deformation between the two dots markers.

Video-metric measurements of PP/EPR film shrinkage

The experiment presented here enables a good qualitative measurement of the polypropylene film dimensional instabilities at the time of thermal treat-

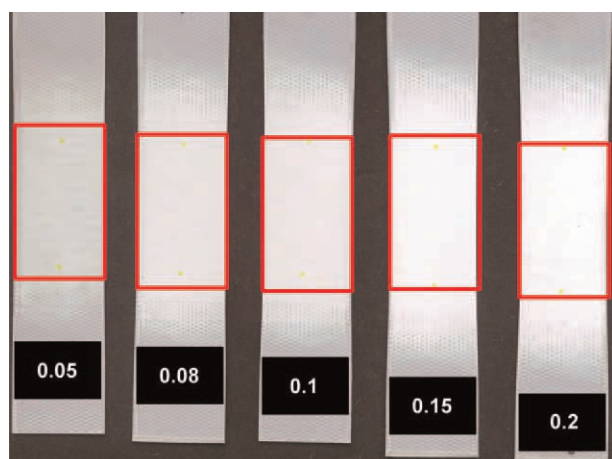


Figure 3 Samples shapes of Film B after deformation to each preselected values. [Color figure can be viewed in the online issue, which is available at wileyonlinelibrary.com.]

ments. It was devised and developed at the Département SI2M (Science et Ingénierie des Matériaux et Métallurgie) of the Institut Jean Lamour (Ecole Nationale Supérieure des Mines de Nancy). The equipments save data which enables to provide good representation of the phenomenon. Influences of parameters such as annealing temperature, heating rate, macromolecular chains orientation, and predeformation at constant true deformation rate can be studied. The experimental setup of this new experience is described below.

The system consists in dots markers displacements measurements in function of temperature and time. The heating plate used enables temperature scans at velocities in the range of 6–90°C min⁻¹ and annealing at various temperatures with a precision of 1°. It is commercialized by Harry Gestigkeit GmbH (Düsseldorf) under the reference PZ28-2. Before the beginning of the test a number of points (about 150) are judiciously placed onto the polymer coating as shown by the experimental set up schematized in Figure 4. The mixture used to create these points is based on a specific solution of latex and phosphorescent particles diluted in solvent.⁵ Displacements can be followed live with temperature and time using an UV lamp, a CCD camera with black and white contrast, and a program computer which enables to calculate centres of mass of each dot marker.⁵

Dots makers are disposed all over the surface of the organic layer to get displacements of at least each millimetre of the sample. Attention is laid on the importance of a dot marker precisely placed right in the middle of the polymer film. As shrinkage is a symmetrical phenomenon, this dots marker will play the role of reference for numerical posttreatment of the experimental data. Thus, displacements

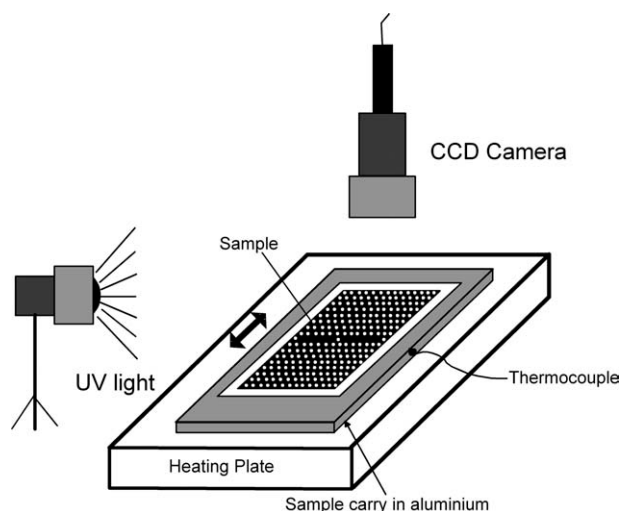


Figure 4 Experimental setup of the video-metric measurements system (the arrow represents the extrusion flow direction of the organic layer).

profiles are obtained with position ($x = 0$, $y = 0$) defined as the middle of the sample. Experimental errors on displacements measurements are evaluated to 0.5 mm.

To improve heat transfer and then to ensure a good temperature measurement of the organic film, a carry sample made in aluminum is used with a silicon-based heat transfer compound. The thermocouple is placed inside the aluminum piece just under the steel blade (Fig. 4). Finally we got an organic film temperature control of $\pm 1^\circ\text{C}$.

Raman spectroscopy measurements of PP/EPR shrinkage

Many authors^{1,6,17,18} have exposed an effective method that permits to estimate the macromolecular chains orientation of various polymer such as isotactic polypropylene using Raman spectroscopy in back scattering mode. To quantify the macromolecular orientation along the thermal test, the incident laser is polarized parallel to the machining direction. This method consists in the study of the evolution of a spectral characteristic band region of the PP/EPR in the range of $750\text{--}1020\text{ cm}^{-1}$. Attention is especially laid on the evolutions of the bands 973 and 998 cm^{-1} . The first one is mainly assigned to the asymmetric stretching of the axial C-C bond from the crystalline phase. The second one characterizes the rocking of the ($-\text{CH}_3$) lateral group. Thus, depending on the incident laser polarization parallel to the reference direction and the isotropic or anisotropic state of the polymer samples, the evolution of the ratio $I(973\text{ cm}^{-1})/I(998\text{ cm}^{-1})$ gives information about the macromolecular chains orientation of the analyzed sample.⁶

Another specific spectral region gives information about the microstructure of the polymer. The band at 835 cm^{-1} is characteristic of the C-C bond vibration of the amorphous region of the semi-crystalline material. So, its normalized (to the spectra global intensity) peak intensity measurement informs about the amount of melting phase present in the material. As a consequence, it is possible to observe the progressive melting of the organic film during the heating.

The apparatus used is a LabRam micro-spectrometer developed by Horiba-Jobin Yvon (Lille, France) equipped with the Olympus confocal microscope and motorized x - y table. Spatial resolution approaches 1.2 cm^{-1} and the network range is $700\text{--}1800\text{ cm}^{-1}$. Measurements are done with the acquisition software Labspec®. The optic objective used is $50\times$ with large focal. The laser wavelength is 785 cm^{-1} and corresponds to a red laser diode. Power illumination on polymer samples is 12 mW . Spectra are fitted using a fitting list square procedure based

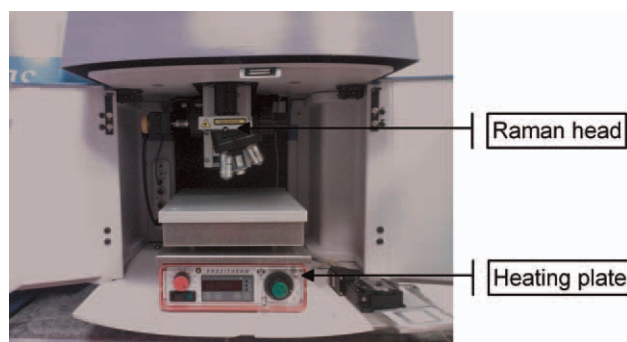


Figure 5 Apparatus of the *in situ* Raman measurements of shrinkage. [Color figure can be viewed in the online issue, which is available at wileyonlinelibrary.com.]

on Lorentzian function adjustments. The analysis depth is $20\text{ }\mu\text{m}$ with a pinhole aperture of $150\text{ }\mu\text{m}$ width.

The experimental setup seems like the one exposed previously in the Samples Preparation part of this article. The main differences are that no more dots markers are disposed on the polymer surface and that the UV lamp and the CCD camera are replaced by a Raman head (Fig. 5). The chosen heating rate is 6°C min^{-1} to let enough time to perform proper Raman acquisition (20 s .) and to keep close to the industrial conditions described later in Influences of the Heating Mode part of this manuscript.

Shrinkage measurements of prestrained samples

The mechanical behavior of the metal/polymer composite stretched uniaxially is obtained at the ambient temperature for a constant true deformation rate of $5 \times 10^{-3}\text{ s}^{-1}$. True deformation values are controlled live by the VideoTraction™ system in the two dots markers mode [Fig. 2(b)].⁵ Between these two points, it is assumed that the deformation is homogenous and can be calculated using Lagrangian interpolation of each point displacement. Indeed, plastic necking for steel keeps weak until fracture. This is the reason why we can assume the deformation value measured between the two dots markers as equal to a local true strain: $\varepsilon = \ln(l/l_0)$. Five predeformation values are chosen to characterize the whole range of the mechanical composite life in plane tensile mode: 0.05 , 0.08 , 0.1 , 0.15 , and 0.2 (Figs. 3 and 6). For all shrinkage experiments on the influence of a sample predeformation, heating rate was always $75^\circ\text{C min}^{-1}$.

EXPERIMENT RESULTS

Influences of the heating mode

At the car manufacturers, the kinetic of the cataphoresis process consists in a constant increase of

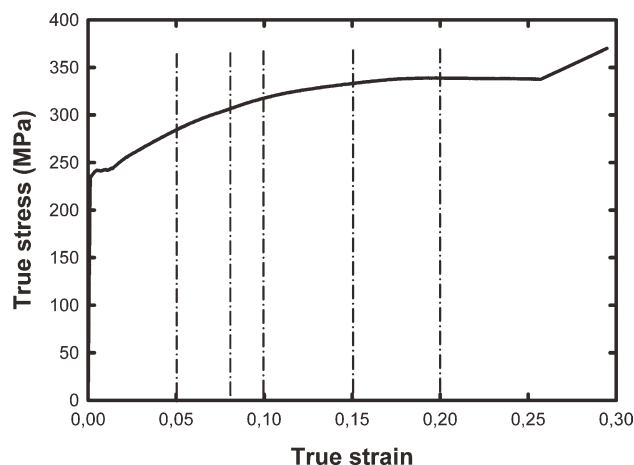


Figure 6 Illustration of the selected predeformation on the composite true mechanical behavior in plane tensile test ($T = 25^{\circ}\text{C}$, $\dot{\epsilon} = 5 \times 10^{-3} \text{ s}^{-1}$).

temperature from 25 to 160°C at an average rate of $22^{\circ}\text{C min}^{-1}$. Then from 160 to 200°C , the heating velocity is about $6^{\circ}\text{C min}^{-1}$. Pieces stay at this highest temperature for 20 min. The cooling takes place in air at an average rate of $35^{\circ}\text{C min}^{-1}$. The important data for our study is the heating rate at which the

PP/EPR layer melts: $6^{\circ}\text{C min}^{-1}$. That is the reason why we will present the influences of heating rate (in the range $6\text{--}75^{\circ}\text{C min}^{-1}$), and temperature and time of annealing for the initially oriented Film A (orientation induced by the extrusion process).

Influences of the heating rate

Figure 7 presents an experimental shrinkage illustration of Film A heated at 6 and $75^{\circ}\text{C min}^{-1}$ [Fig. 7(b,c), respectively]. Actually, Figure 7(b,c) only enlighten the shrinkage of one quarter of the whole sample as explained by the Figure 7(a) because of the radial symmetry of the phenomenon with respect to the centre of the sample. These results put in evidence that no measurable shrinkage occurs in the transversal direction of the extrusion flow (“y” axis). On the contrary, along the machining direction (“x” axis), the polymer film moves during the heating. Furthermore, we can notice that the distance from the edge (position: $x = 15$, y) to the sample centre (position: $x = 0$, $y = 0$) where polymer shows motion during the thermal test increases when the heating rate is slower. Indeed, we can notice a displacement zone of the matter which is bigger for the

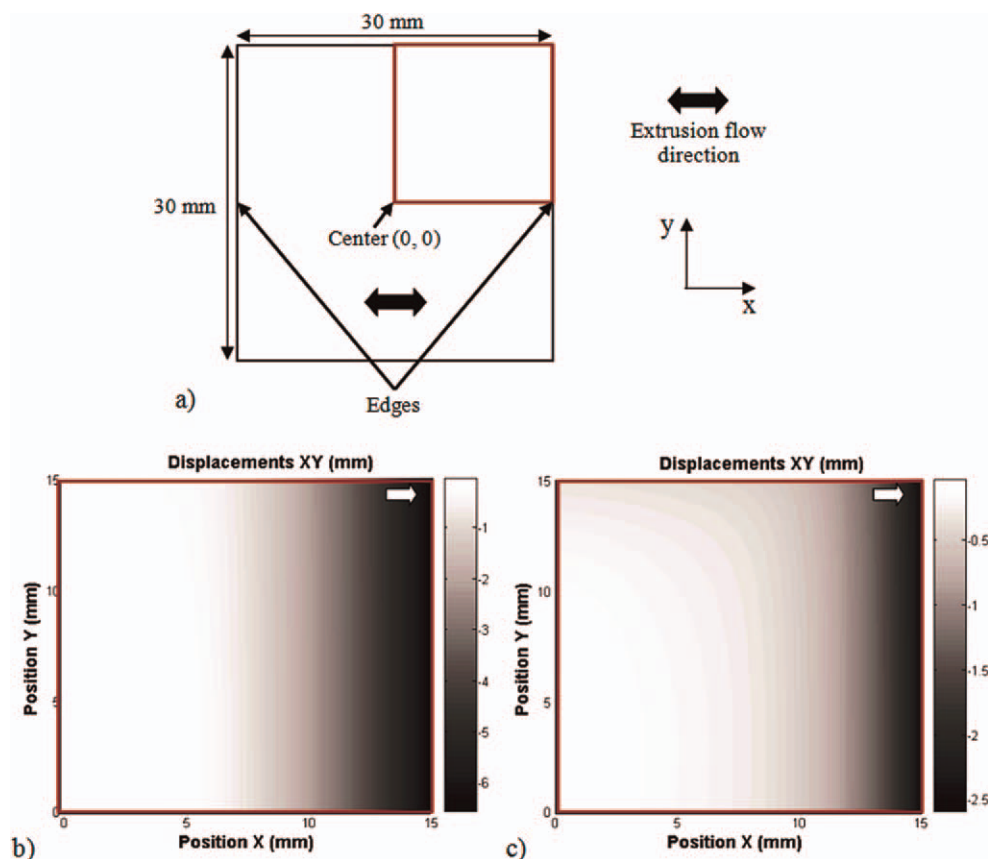


Figure 7 (a) Geometrical description of the samples. Position ($x = 0$, $y = 0$) is the sample centre which keeps motionless all along the thermal test. The white arrow indicates the extrusion flow direction. The red square represents the area where the displacement profile in case of Film A is measured and illustrated for shrinkage tests at (b) $6^{\circ}\text{C min}^{-1}$, and (c) $75^{\circ}\text{C min}^{-1}$. [Color figure can be viewed in the online issue, which is available at [wileyonlinelibrary.com](http://www.interscience.wiley.com).]

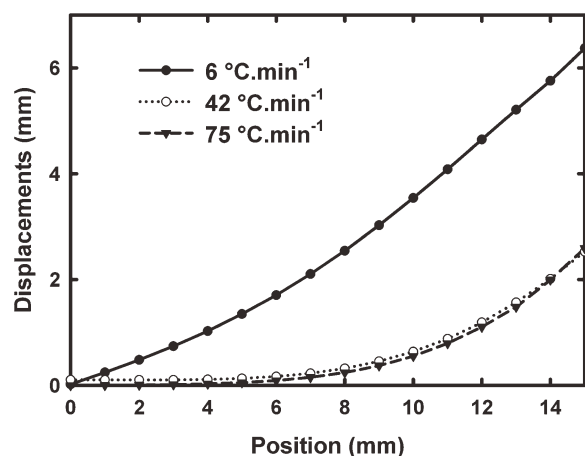


Figure 8 Film A displacements profile in function of the heating rate.

test at the lower heating rate (larger gray zone on Fig. 7). Figure 8 which also presents heating rate influences on shrinkage magnitude of the pre-oriented Film A shows that for a heating rate of $75^{\circ}\text{C min}^{-1}$, almost 9 mm from the centre of the sample do not present motion of matter whereas at $6^{\circ}\text{C min}^{-1}$, only 2 mm from the central position is motionless. According to these results, important differences appear. At $6^{\circ}\text{C min}^{-1}$, the shrinkage magnitude, in terms of maximal displacements of the sample edges ($x = 15 \text{ mm}$), is three times higher than at $42^{\circ}\text{C min}^{-1}$. The uncovered bear part distance is equal to 6.4 mm in the extrusion flow direction. Moreover, we observe that above $42^{\circ}\text{C min}^{-1}$ shrinkage value keeps constant and independent of the heating rate.

Figure 9 enlightens the heating rate influence on melting behavior of the organic layer. The adhesive polymer does not induce signal in thermograms due to its weak proportion which represents less than 15% of the global thickness. DSC results of Figure 9

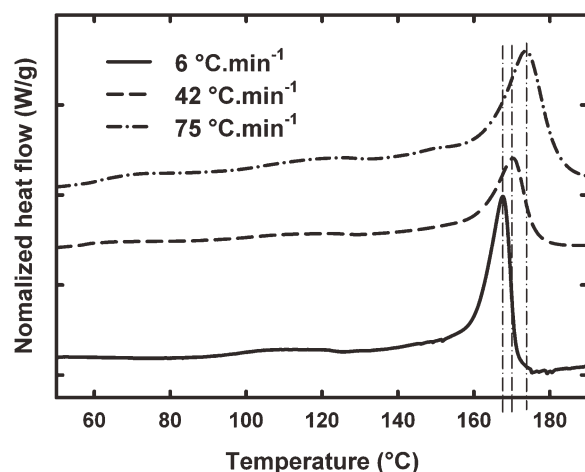


Figure 9 Influences of the heating rate on the Film A melting behavior.

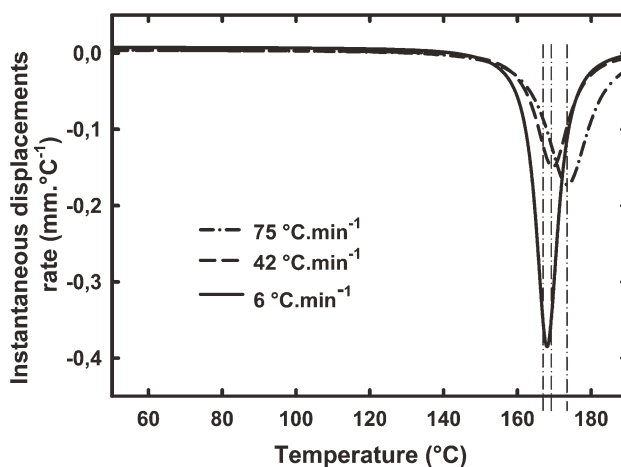


Figure 10 Film A instantaneous displacements rate profile of the edge of Film A in function of the heating rate.

show that melting temperatures taken at the endothermic maximum depend on the heating rate. At $6^{\circ}\text{C min}^{-1}$, majority size crystalline lamellae melts at 167°C whereas at $42^{\circ}\text{C min}^{-1}$ it happens at 169°C and at $75^{\circ}\text{C min}^{-1}$, it occurs at 174°C . Figure 10 presents the evolution of the instantaneous displacements rate for all two degrees Celsius during the heating treatment; these temperatures correspond to the maximum of shrinkage. It can be also noticed that the onset and the end temperatures revealed by DSC correspond to the initiation and the end of the shrinkage phenomenon.

For high speed heating superior to $42^{\circ}\text{C min}^{-1}$, final state of the sample is schematized on the Figure 11. Three characteristic zones can be enlightened: (A)

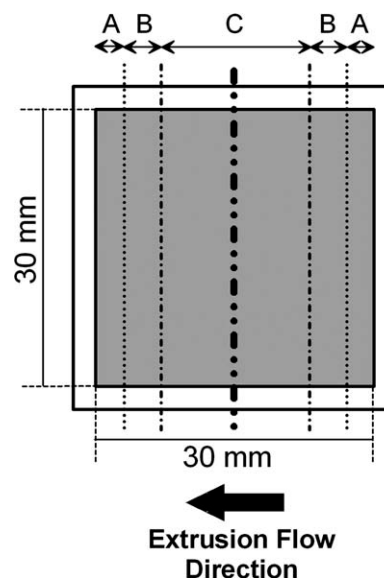


Figure 11 Typical displacement profile: (A) uncovered bear parts, (B) measurable displacements zone, and (C) static zone.

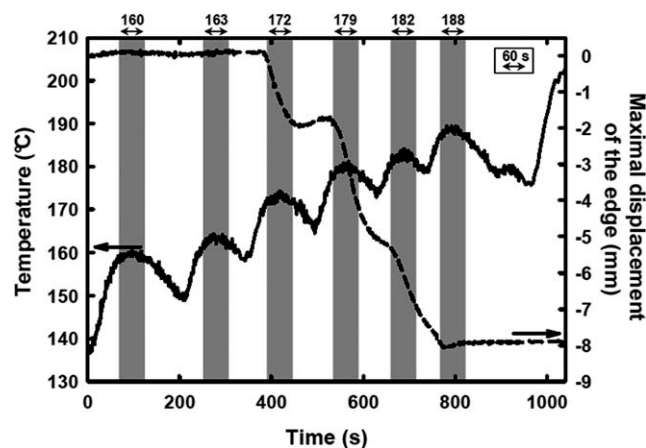


Figure 12 Film A maximal displacements values in case of successive annealing of 1 min at temperatures around the shrinkage range (160, 163, 172, 179, 182, 188°C). Heating rates to reach each program temperature are equal to $(20 \pm 3)^\circ\text{C min}^{-1}$.

uncovered bear parts where steel is exposed to environmental degradation, (B) measurable displacements zone (the matter moves but does not uncover the steel blade), and (C) static zone where no matter motion is measured. In case of oriented film, this schema is always true whatever the thermal proceeding applied to the sample. Only their dimensions may change in function of the heating rate as shown earlier by the Figures 7 and 8.

Influences of temperature and time of annealing

This study focuses the influences of temperature and time of various annealing on the thermal shrinkage. First, we proceed to six short annealing of 1 min characterized by a heating rate of $(20 \pm 3)^\circ\text{C min}^{-1}$ between each temperature. They are 160, 163, 172, 179, 182, and 188°C. In case of Film A, Figure 12 presents the thermal program in function of time of the applied annealings. The evolution of the sample edge displacement (maximal polymer displacement inducing uncovered bear parts of steel) in the extrusion flow direction for each annealing is juxtaposed. As previously these displacements are calculated taking the sample middle point as a reference. Once the thermal cycle is over, the maximal displacement (of the sample edges in the machining direction) which induces uncovered steel is equal to 8 mm. As shown before, no significant shrinkage occurs for temperatures below the melting point (160 and 163°C). Annealing at 172°C starts the phenomenon. For 1 min, 25% of the total shrinkage takes place. The decrease in temperature before the next step instantaneously stops displacements. Then at 179°C, the 1 min annealing induces 37.5% of the final shrinkage value. In the same manner, it stops when

temperature decreases. All the rest of the polymer layer displacement takes place at 182 (31.5%) and 188°C (6%). Finally, the increase until 200°C does not change the final value of shrinkage.

Then, we realize a long time annealing of 40 min at 169°C, just below the starting temperature revealed previously. Results are exposed on Figure 13. Heating rates are superior to $42^\circ\text{C min}^{-1}$ for these two isothermal treatments. So, as seen before, it means that the heating rate influence is identical for the two tests. No displacements and consequently no shrinkage significantly appear (<0.5 mm). On the contrary, 40 min at 180°C induces shrinkage of about 7.5 mm. However, the main part of the sample edge displacement occurs after the first 5 min. Then, no more changes appear during the 35 min left.

Influences of the initial crystalline orientation

In this section, we will present results on the importance of the thermomechanical history induced by the transformation process (extrusion) of our samples on the shrinkage magnitude. This way, we compare two Films (A and B) which do not have the same initial degree of macromolecular chains orientation along the machining direction (Table I). Film A has been obtained by extrusion followed by calendering as cooling postextrusion process, and Film B has been processed by cast extrusion. Wide angle X-ray scattering in transmission mode gives patterns which enable the determination of the polymer film crystalline texture. Hermans crystalline orientation factor for each film is calculated taking the extrusion flow direction as reference. Results are -0.22 and -0.06 , respectively for Film A and Film B (Table I). Therefore, Film A presents its crystalline macromolecular chains much more oriented in the flow extrusion direction than those of Film B. Table II gathers

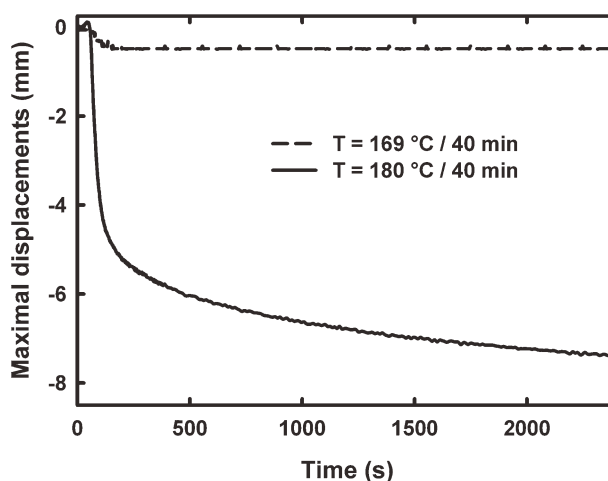


Figure 13 Influence of annealing times on shrinkage of Film A. The heating rates are superior to $42^\circ\text{C min}^{-1}$.

TABLE II
Influence of the Crystalline Orientation on Shrinkage Values in Function of Heating Rates

Films names	6°C min ⁻¹	75°C min ⁻¹
A	6.4 mm	2.6 mm
B	0.6 mm	0.4 mm

all the shrinkage tests results obtained for two different heating rates (6 and 75°C min⁻¹). It appears that no shrinkage occurs when the macromolecular chains distribution is isotropic in the film plane whatever the heating rate is.

Coupling the Raman spectrometer to the heating plate, the evolution of the ratio $I(973\text{ cm}^{-1})/I(998\text{ cm}^{-1})$ is calculated all along the heating from the ambient temperature to 200°C at 6°C min⁻¹.⁶ Figure 14 shows that Films A and B initially do not have the same crystalline orientation degree due to their different ratio values. This result confirms the one illustrated by the Hermans orientation factor deduced from WAXS analysis (Table I). In function of temperature, this ratio decreases between 155 and 175°C with an inflection point at 167°C for both films. In the same way, the evolution of the spectral band characteristic of the amorphous region (835 cm⁻¹) informs us on the polymer melting. It begins at 160°C and ends at 172°C. The inflection point is also located at 167°C. Similar results are obtained with Film A [Fig. 14(a)] and Film B [Fig. 14(b)]. The both inflection points correspond to the melting temperature measured at 6°C min⁻¹ by differential scanning calorimetry (Fig. 9).

Influences of a controlled prestrain on samples

As enounced previously in the Experimental part of this article, five predeformation values were chosen to study mechanical influences on the shrinkage

phenomenon at the heating rate of 75°C min⁻¹. Figures 15 and 16 show displacement and deformation profiles along the semi-length of the sample (shrinkage is assumed symmetrical regarding the sample centre) in case of Film B and A, respectively.

Film B is initially not oriented which means that the extrusion process did not induce internal stress concentrations and/or macromolecular texture. So, no shrinkage occurs at 0 of deformation during the thermal treatment. However, regarding Figure 15, the shrinkage magnitude increases with the deformation value. For the maximum predeformation of 0.2, results show a maximal displacement of the edge of about 1 mm. We can notice that this value increases linearly with the deformation from 0 to 0.2. The deformation curves [Fig. 15(b)] deduced from these displacements results using Lagrangian interpolation show also a proportional increase in function of the prestrain. At the position 0 mm, the deformation values are not null due to the inexistence of a motionless zone in the prestrained sample. Only the exact middle of the samples does not move due to the symmetrical aspect of the shrinkage phenomenon.

Film A is initially oriented due to a bad set of extrusion process parameters. Figure 16 presents results of the modifications of shrinkage magnitude due to previous deformation done by plane tensile tests. Only the largest prestrain value was studied (0.2). We notice an increase of shrinkage of about 1.3 mm. From the deformation curves [Fig. 16(b)], it is easy to observe the motionless zone in case of film oriented during its elaboration. After deformation, this zone disappears.

Figure 17 shows Film A maximal shrinkage displacement profile (edge of the sample) without and with predeformation of 0.2. The first observation is that the phenomenon beginning temperature in case of prestrained sample (0.2) appears earlier than for

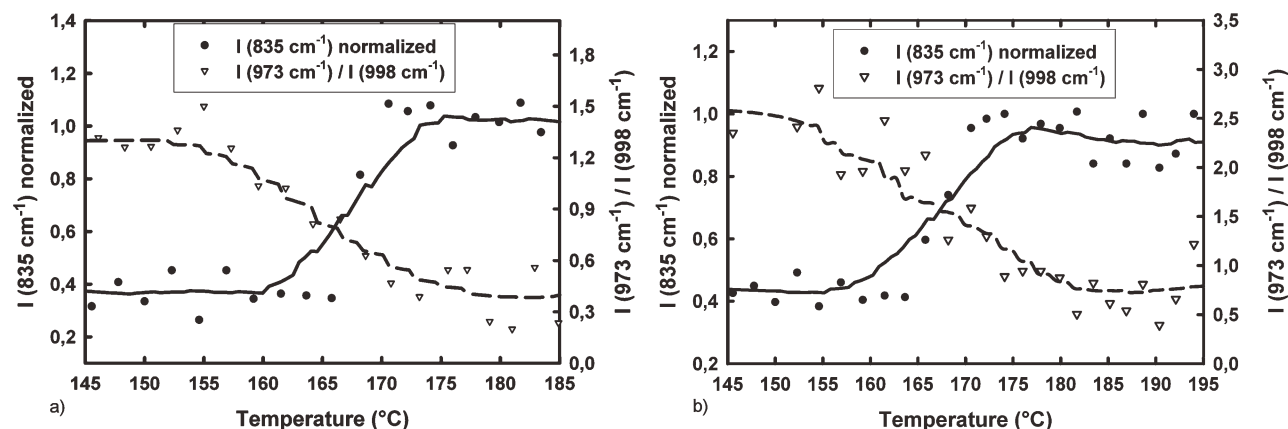


Figure 14 Melting and crystalline disorientation measured by Raman spectroscopy of (a) Film A and (b) Film B in function of temperature ($v_{\text{heating}} = 6^\circ\text{C min}^{-1}$).

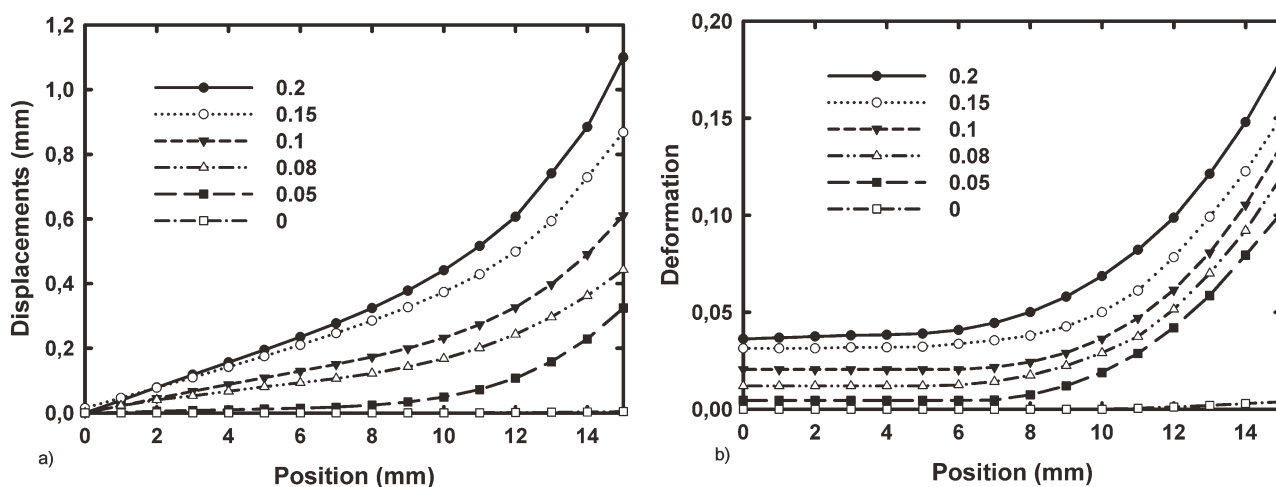


Figure 15 (a) Displacements profile and (b) deformation profile of Film B in function of predeformation values.

unstrained sample. Displacements take place at 138°C instead of 162°C. The 138°C is higher of 2°C to the melting point of the adhesive layer. At this temperature, the upper polymer did not start melting ($T_m = 167^\circ\text{C}$). So, we can attribute these first displacements to the healing of the volume damage induced during the tensile test. Until 155°C, shrinkage magnitude is equal to 1.1 mm. Then, the remaining 2.8 mm can be divided in two micro-structural contributions: 2.6 mm are due to the initial crystalline orientation induced by the conformation process, and 0.2 mm to the predeformation. This last part is in good agreement with our previous structural studies on the degree of crystalline orientation developed during a tensile test.¹

DISCUSSION

As a result of the manufacturing process, internal stresses may be locked during cooling inside the

microstructure of a polymer film. They can be released by heating. The temperature, at which shrinkage will occur, and its magnitude depends on the processing techniques employed to produce the film. Main results show strong influences of the initial crystalline orientation induced by the film extrusion process and of the sample stretching in case of stamping, for instance. Moreover, heating modes show great influences on the final magnitude of shrinkage.

As described by the Figure 9 in case of pre-oriented samples, typical DSC melting temperatures revealed by the endothermic signal are $T_{\text{onset}} = 157^\circ\text{C}$, $T_{\text{end}} = 170^\circ\text{C}$, and $T_m = 167^\circ\text{C}$ at 6°C min^{-1} . At the same heating rate, they coincide with the initiation, the stop, and the maximal instantaneous displacement of the shrinkage phenomenon. So, instabilities only result from the crystalline microstructure melting. Indeed, annealing at temperature just below the melting point does not induce

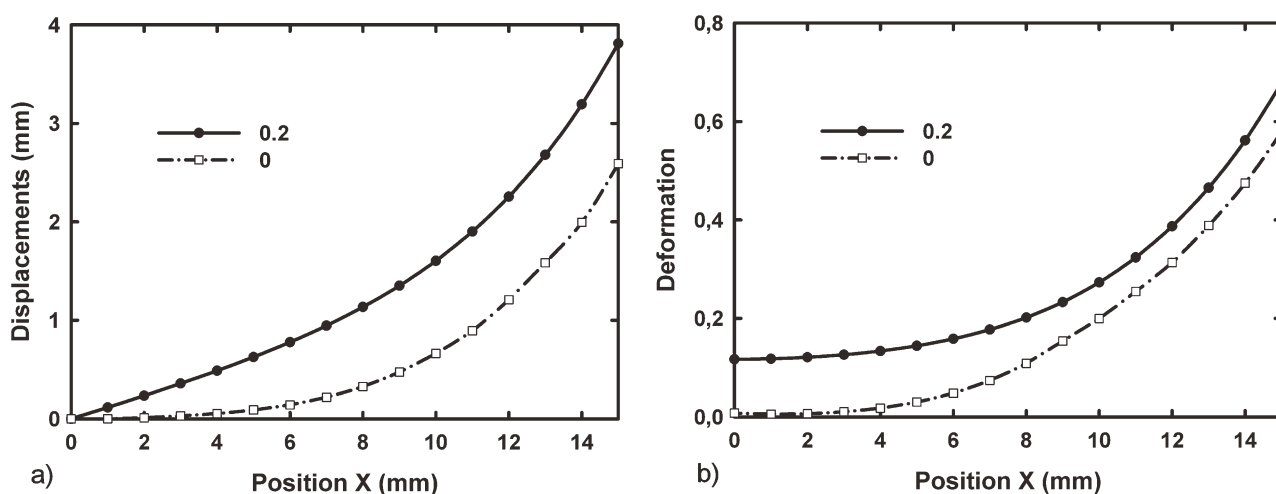


Figure 16 (a) Displacement profile and (b) deformation profile of Film A with and without predeformation of 0.2.

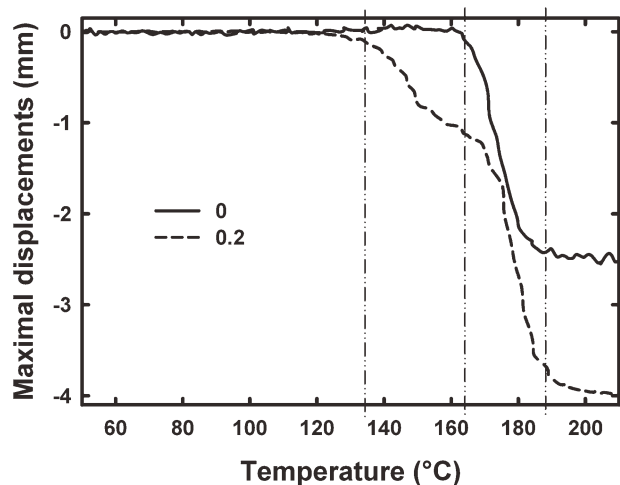


Figure 17 Film A maximal displacement profile (edge of the sample) with and without predeformation of 0.2.

significant shrinkage. As developed by Samuels (1974)¹⁹ and Vries (1982),² the amorphous phase presents a negligible chains orientation compared to the crystalline phase. It means that the amorphous region of the polymer had enough time before the film lamination on steel to relax completely.

By Raman spectroscopy, it is possible to follow live the macromolecular disorientation and the crystalline microstructure melting (Figs. 13 and 14) for unoriented and oriented films. More than a confirmation of DSC observations (T_{onset} , T_{end} , and T_m) at 6°C min^{-1} , Raman results show that even for a material which doesn't present a high initial crystalline texture in the extrusion direction, the melting is characterized by a return to the most stable thermodynamic equilibrium of polymers: the random coil. In this case the decrease of the orientation ratio reveals a preferential macromolecular chains distribution in the film plane.

A tensile predeformation modifies the main characteristics of the shrinkage phenomenon described above. The initiation temperature at $75^\circ\text{C min}^{-1}$ is lower (138°C instead of 162°C) and corresponds to the melting of the adhesive layer. It means that shrinkage is not anymore only involved by stress concentrations locked in the crystalline phase ($T_m = 170^\circ\text{C}$ at $75^\circ\text{C min}^{-1}$). The presence of a steel substrate does not allow the relaxation and the recovery of the amorphous phase because steel is less ductile than polymer. Thus, the disorientation of the macromolecular chains of the amorphous region is limited by a mechanical stress brought by the adhesion of the polymer layer on the steel blade. That is the reason why shrinkage occurs at the time of the adhesive layer melting. At the main melting temperature of the PP/EPR layer of the composite, no more shrinkage appears compared to the same material

without predeformation. We can propose that the additional displacement observed on stretched samples is mainly due to the relaxation and recovery of the amorphous phase and a partial healing of the volume damage.^{1,7}

CONCLUSION

This article presents an experimental study focused on the dimensional instabilities of polypropylene films laminated on steel. This phenomenon, also called shrinkage, is provided from the thermomechanical history of the material. Indeed, the various processes endured during the conformation induce particular semi-crystalline microstructures which are able to relax to a more stable thermodynamic state (random coil) at the time of heating treatments. Videometric measurements coupled with Raman spectroscopy are an innovative way to characterize and analyze *in situ* the shrinkage of such kind of composites. Microstructural mechanisms responsible for these geometrical instabilities can be identified. Without previous stretching, shrinkage takes place when the oriented crystalline macromolecular chains melt. This orientation is due to the extrusion process. The magnitude depends on the kinetic of the thermal treatment because of the bad heat diffusion properties of polypropylene. After a tensile test which only induces voids creation inside the film, shrinkage occurs at lower temperature. It is attributed to the melting of the adhesive layer and the healing of volume deformation developed inside the PP/EPR layer. When temperature approaches the fusion of this last layer, the same shrinkage occurs as in case of an unstretched sample due to the disorientation of the crystallized macromolecular chains.

The authors gratefully acknowledge the kind contribution of the LMOPS (Laboratoire Matériaux Optiques, Photonique et Systèmes of the Université de Metz), and in particular Professor Patrice Bourson, to this article in terms of Raman microscopy measurements.

References

1. Ponçot, M. Comportements Thermomécaniques de Polymères Chargés Selon Différents Chemins de Déformation et Traitements Thermiques. Doctoral thesis of ENMSN/INPL, 2009.
2. Vries, A. J. *Pure Appl Chem* 1982, 54, 647.
3. Baltá-Calleja, F. J.; Peterlin, A. *Die Makromol Chem* 1971, 141, 91.
4. Haudin, J. M.; Piana, A.; Monasse, B.; Monge, G.; Gourdon, B. *Ann Chim Sci Matér* 1999, 24, 555.
5. G'sell, C.; Hiver, J. M.; Dahoun, A. *Int J Sol Struct* 2002, 39, 3857.
6. Martin, J.; Ponçot, M.; Bourson, P.; Dahoun, A.; Hiver, J. M. *Polym Eng Sci* 2011, 51, 1607.
7. Pawlak, A.; Galeski, A. *J Polym Sci B* 2010, 48, 1271.

8. Pomerleau, J.; Sanschagrín, B. *Polym Eng Sci* 2006, 10, 1275.
9. Régner, G.; Trotignon, J. P. *Polym Test* 1993, 12, 383.
10. Jansen, K. M. B.; Van Dijk, D. J.; Husselman, M. H. *Polym Eng Sci* 1998, 38, 838.
11. Hoff, M.; Pelzbauer, Z. *Polymer* 1991, 32, 3317.
12. Tunnicliffe, J.; Blundell, D. J.; Windle, A. H. *Polymer* 1980, 21, 1259.
13. Mae, H.; Omiya, M.; Kishimoto, K. *J Solid Mech Mater Eng* 2008, 2, 1018.
14. Moore, E. *Polypropylene Handbook*; Hanser: Munich, 1996.
15. Hermans, J. J.; Hermans, P. H.; Vermaas, D.; Weidinger, A. *Rec Trav Chim (Pays-Bas)* 1946, 65, 427.
16. Hermans, P. H.; Weidinger, A. *J Appl Phys* 1948, 19, 491.
17. Arruebarrena de Baez, M.; Hendra, P. J.; Judkins, M. *Spectrochim Acta A* 1995, 51, 2117.
18. Hendra, P. J.; Cutler, D. J.; Sang, R. *Faraday Discuss Chem Soc* 1979, 68, 320.
19. Samuels, R. J. *Structured Polymer Properties: The Identification, Interpretation and Application of Crystalline Polymer Structure*; Wiley: New York, 1974.